

## Articles

---

### The Murine Anti-Human Common $\gamma$ Chain Monoclonal Antibody CP.B8 Blocks the Second Step in the Formation of the Intermediate Affinity IL-2 Receptor

Darren P. Baker,\* Adrian Whitty, Mohammad R. Zafari, Dian L. Olson, Catherine A. Hession, Konrad Miatkowski, Lena S. Avedissian, Susan F. Foley, Michele L. McKay, Christopher D. Benjamin, and Linda C. Burkly

*Biogen Inc., 14 Cambridge Center, Cambridge, Massachusetts 02142*

*Received June 9, 1998; Revised Manuscript Received July 23, 1998*

**ABSTRACT:** A murine monoclonal antibody, CP.B8, specific for the extracellular portion of the human common  $\gamma$  ( $\gamma_c$ ) chain, and its Fab fragment are shown to block the binding of IL-2 to COS-7 cells transfected with the cDNA for the full-length IL-2 receptor  $\beta$  (IL-2R $\beta$ ) and  $\gamma_c$  chains, components which together comprise the intermediate affinity IL-2 receptor (IL-2R) expressed on the surface of resting T cells, NK cells, and on certain intestinal epithelial cells. To investigate the mechanism of this inhibition, the extracellular portions of the IL-2R $\beta$  and  $\gamma_c$  chains were expressed and purified, and their interactions with each other and with IL-2 were studied by gel filtration and by surface plasmon resonance (SPR). By gel filtration, a stable ternary complex was formed by association of the three proteins, while no stable binary complexes were detected between any two of the three proteins. By SPR analysis, IL-2 was shown to associate rapidly with IL-2R $\beta$ , forming a binary complex with an equilibrium dissociation constant ( $K_d$ ) of 800 nM, which permitted subsequent association of the  $\gamma_c$  chain. Dissociation of the IL-2/IL-2R $\beta$ / $\gamma_c$  chain complex was significantly slower than dissociation of the IL-2/IL-2R $\beta$  complex. Using these model systems, we tested the ability of mAb CP.B8 to inhibit the association of the  $\gamma_c$  chain with IL-2 and IL-2R $\beta$ . By gel filtration, mAb CP.B8 formed a stable complex with the  $\gamma_c$  chain, preventing its association with IL-2 and IL-2R $\beta$ . MAb CP.B8 was also capable of dissociating the  $\gamma_c$  chain already complexed with IL-2 and IL-2R $\beta$ . SPR analysis confirmed these findings and showed, in addition, that the Fab fragment of CP.B8 was also capable of inhibiting the association of the  $\gamma_c$  chain with the IL-2/IL-2R $\beta$  complex. We conclude that mAb CP.B8 blocks the second step in the formation of the intermediate affinity IL-2R on the surface of transfected COS-7 cells by binding at or close to a region on the  $\gamma_c$  chain that is involved in contact with IL-2 and/or IL-2R $\beta$ .

The receptors for the cytokines IL-2, IL-4, IL-7, IL-9, and IL-15 share a component called the common  $\gamma$  ( $\gamma_c$ )<sup>1</sup> chain

(I-6) which was first identified as the third subunit of the IL-2R (I). The  $\gamma_c$  chain is expressed on CD4<sup>+</sup> and CD8<sup>+</sup> T cells (7-9), B cells (7), NK cells (7, 8), monocytes (7),

---

\* Corresponding author. E-mail: darren\_baker@biogen.com.

<sup>1</sup> Abbreviations: PBS, 1.5 mM KH<sub>2</sub>PO<sub>4</sub>, 8.1 mM Na<sub>2</sub>HPO<sub>4</sub>, pH 7, 2.7 mM KCl, and 138 mM NaCl; HBS, 10 mM HEPES, pH 7.4, 150 mM NaCl, and 3.4 mM EDTA; IL-2, interleukin-2; IL-2R, interleukin-2 receptor;  $\gamma_c$  chain, common  $\gamma$  chain;  $\gamma_{\text{His}}$ , His-tagged extracellular portion of the common  $\gamma$  chain; BSA, bovine serum albumin; SPR,

surface plasmon resonance; RU, resonance units; PBMC, peripheral blood mononuclear cells; PHA, phytohemagglutinin; PTH, phenylthiohydantoin; cpm, counts per minute; MOI, multiplicity of infection; SDS-PAGE, sodium dodecyl sulfate-polyacrylamide gel electrophoresis; FCS, fetal calf serum; CTL, cytotoxic T lymphocytes.

neutrophils (10), bone marrow, and cord blood CD34<sup>+</sup> progenitor cells (11), as well as on dendritic cells (12) and on certain intestinal epithelial cells (13). The mature protein is a 347 amino acid residue, type I integral membrane protein, and is a member of the hematopoietic receptor superfamily (14). The extracellular portion of the  $\gamma_c$  chain contains two fibronectin type III-like domains which, in addition to being involved in cytokine binding, may also play a role in cell adhesion and signaling through activated  $\beta 1$  integrins (15). The importance of the  $\gamma_c$  chain as a functional constituent of multiple interleukin receptors is underscored by the severity of immunodeficiency often associated with mutations in the  $\gamma_c$  chain gene (16, 17). The resulting syndrome, X-linked severe combined immunodeficiency (XSCID), is characterized by the absence, or presence of only very low levels, of T and NK cells (18). Mutations found in patients with XSCID occur in both the extracellular and cytoplasmic portions of the protein, resulting in impaired cytokine binding and/or in cytokine-mediated signal transduction (17, 19–23). In addition to the role that the  $\gamma_c$  chain plays in thymic development (24, 25), the protein is also required for mature T cell proliferation (2).

Of the  $\gamma_c$  chain-dependent cytokine receptors, the IL-2R is the most studied. On antigen-activated T cells, high-affinity binding of IL-2 ( $K_d = 10$  pM) (26) is dependent upon the association of the IL-2R $\alpha$ , IL-2R $\beta$ , and  $\gamma_c$  chains, while signal transduction, mediated by the activation of JAK1 and JAK3 kinases (5), is dependent specifically upon the association of the cytoplasmic portions of the IL-2R $\beta$  and  $\gamma_c$  chains (27–29). By contrast, the functional IL-2R on resting T cells is the intermediate affinity complex ( $K_d = 1$  nM) (26) formed by the constitutively expressed IL-2R $\beta$  and  $\gamma_c$  chains without participation of the IL-2R $\alpha$  chain. While IL-2 alone cannot promote proliferation of resting T cells (30), binding of IL-2 to the intermediate affinity IL-2R has been shown to protect resting T cells from radiation-induced death (31). Moreover, both IL-4 and IL-7, whose receptors utilize the  $\gamma_c$  chain, also protect resting T cells from radiation-induced death, while IL-1, IL-3, and IL-6, whose receptors do not utilize the  $\gamma_c$  chain, are not protective (31). In addition to its role on resting T cells, the intermediate affinity IL-2R $\beta$ / $\gamma_c$  complex is the functional IL-2R on NK cells (32, 33) and on certain intestinal epithelial cells (13).

Since the intermediate affinity IL-2R $\beta$ / $\gamma_c$  complex is an important form of the IL-2R, not only in itself but also as the core signaling unit of the IL-2R $\alpha$ /IL-2R $\beta$ / $\gamma_c$  high-affinity complex, it was of significant interest to determine whether the function of the receptor could be inhibited by specifically blocking the association of the  $\gamma_c$  chain with the IL-2R $\beta$  chain in the presence of IL-2. Although a small molecule inhibitor based on the structure of IL-2 has been shown to inhibit the association of IL-2 with the IL-2R $\alpha$  chain (34) and mAbs directed against the IL-2R $\alpha$  chain are undergoing clinical investigation as immunosuppressants (35, 36), antagonists of this type are expected to block the function of only a single cytokine since they are targeted against either the cytokine itself or against the cytokine-specific receptor chain. By contrast, antagonists directed against chains which are shared between cytokine receptors raise the possibility of more effective immunomodulation since they would be expected to simultaneously block the action of multiple cytokines.

Here we report that the binding of IL-2 to the intermediate affinity IL-2R on the surface of COS-7 cells can be blocked by a mAb, CP.B8, directed against the extracellular portion of the  $\gamma_c$  chain. We have characterized the interactions of the extracellular portions of the IL-2R $\beta$  and  $\gamma_c$  chains with each other and with IL-2 using gel filtration and SPR, and we have used these systems to establish the mechanism by which mAb CP.B8 inhibits complex formation.

## EXPERIMENTAL PROCEDURES

**Materials.** Tris, mono- and disodium hydrogen phosphate, and EDTA were purchased from Fisher Scientific; Sf900 II serum-free insect cell medium was purchased from Life Technologies Inc.; Ni<sup>2+</sup>-NTA agarose was purchased from Qiagen; cyanogen bromide-activated Sepharose 4B, imidazole, leupeptin, benzamidine, and pepstatin were purchased from Sigma; aprotinin and protease-free (fraction V) BSA were purchased from Boehringer Mannheim; HEPES was purchased from U.S. Biochemicals; AEBSF was purchased from Calbiochem; disuccinimidyl glutarate, immobilized papain, and cysteine-HCl were purchased from Pierce Chemical Co.; CM5 sensor chips, surfactant P20, amine coupling reagents containing *N*-hydroxysuccinimide, *N*-ethyl-*N'*-(3-diethylaminopropyl)carbodiimide, and ethanolamine-HCl were purchased from BIAcore Inc.

Human [<sup>125</sup>I]IL-2 was purchased from New England Nuclear. Recombinant human IL-2, purified and refolded as described (37, 38), and the derivative of the pBlueBac II baculovirus expression vector encoding the cDNA for the extracellular portion of the human IL-2R $\beta$  chain (39) were kindly provided by Dr. Thomas Ciardelli, Dartmouth Medical School.

**Antibodies.** The murine IgG<sub>1</sub> isotype control MOPC 21 was purified from a hybridoma culture supernatant using Protein A Fast Flow Sepharose (Pharmacia, Piscataway, NJ). The murine IgG<sub>1</sub> anti-human  $\gamma_c$  chain mAb CP.B8 (40) was prepared under contract by Berkeley Antibody Co. (Richmond, CA) from mouse ascites fluid, and was purified by Protos Immunoresearch (San Francisco, CA) using Protein A Fast Flow Sepharose (Pharmacia). The murine anti-human IL-2R $\beta$  chain mAb 18741D was purchased from Pharmingen.

**Expression and Purification of the Extracellular Portion of the Human IL-2R $\beta$  Chain.** The soluble, extracellular portion of the human IL-2R $\beta$  chain, truncated at the junction between the extracellular and transmembrane portions [residues 1–214 of the published sequence (41)], was expressed in *Trichoplusia ni* (High Five) insect cells. A 6.4 L culture of cells grown to a density of  $2.6 \times 10^6$  cells/mL in Sf900 II medium at 28 °C was infected with the derivative of the pBlueBac II (Invitrogen, Carlsbad, CA) baculovirus expression vector encoding the IL-2R $\beta$  cDNA at a multiplicity of infection (MOI) of 5 virions/cell. Fresh Sf900 II medium (1.5 L) was added at the time of infection, and the culture was harvested 48 h postinfection. Cells and debris were removed by centrifugation, the cell-free supernatant (8.6 L) was mixed with 344 mL of 0.5 M Na<sub>2</sub>HPO<sub>4</sub>, pH 8.6, to adjust the pH to between 6 and 7, and the protease inhibitors AEBSF, benzamidine, leupeptin, aprotinin, and pepstatin were added to final concentrations of 200  $\mu$ M, 1 mM, 10  $\mu$ g/mL, 10  $\mu$ g/mL, and 1  $\mu$ g/mL, respectively. The supernatant was then filtered through a 0.45  $\mu$ m filter before being

concentrated to 600 mL by ultrafiltration with a S1Y10 spiral membrane cartridge (Amicon, Danvers, MA). The concentrate was stored at  $-70^{\circ}\text{C}$ . Typically, the protein was purified from 40 mL of the concentrated medium by affinity chromatography using a 1.4 mL column of Sepharose 4B to which the murine anti-human IL-2R $\beta$  mAb 18741D had been coupled at a density of 6.2 mg of antibody/mL of swollen gel. The bound IL-2R $\beta$  was eluted with 0.2 M acetic acid, pH 3, 0.2 M NaCl, and collected as 800  $\mu\text{L}$  fractions into tubes containing 200  $\mu\text{L}$  of 0.1 M Tris-HCl, pH 9, to neutralize the acidity. Fractions identified as containing the protein by absorbance measurements at 280 nm and by reducing SDS-polyacrylamide gel electrophoresis (SDS-PAGE) were pooled, dialyzed extensively against phosphate-buffered saline (PBS),<sup>1</sup> concentrated to approximately 1 mg/mL, filter sterilized, and stored at  $4^{\circ}\text{C}$ . The N-terminal sequence, AVNGTSQFT(C)FYNSR, agreed with the published sequence (41), although Cys at position 10 could not be identified since the protein was not modified prior to sequencing.

**Cloning, Expression, and Purification of the Extracellular Portion of the Human  $\gamma_c$  Chain.** The DNA sequence encoding the extracellular portion of the human  $\gamma_c$  chain, truncated at the junction between the extracellular and transmembrane portions [residues 1–254 of the published sequence (1)], with a hexahistidine tag at the C-terminus (referred to hereafter as  $\gamma_{\text{His}}$ ), was cloned from a Jurkat cDNA library by screening with oligo 310-09 which is antisense to nucleotides 592–620 of the human  $\gamma_c$  chain gene (Genbank accession number D11086). Two clones were sequenced and both were found to have a T at position 673 instead of a C; therefore, the protein has a methionine at position 220 instead of a threonine as published (1). However, this encoded form of the  $\gamma_c$  chain is functionally competent as measured by its ability to mediate high-affinity IL-4 binding when cotransfected into COS-7 cells with the IL-4R $\alpha$  chain, resulting in a  $K_d$  of  $200\text{ pM} \pm 100\text{ pM}$ ,<sup>2</sup> an affinity approximately 3-fold higher than that mediated by the IL-4R $\alpha$  chain alone and in agreement with published results (3). In addition, the encoded  $\gamma_c$  chain mediated IL-2 binding when cotransfected with the IL-2R $\beta$  chain with a  $K_d$  of approximately 1 nM (40), also in good agreement with published results (26). One of these clones, 4A1, was used for production of the His-tagged construct. The His-tagged construct was cloned by PCR with primer 310-08 (5' GCGGCCGCGAAGAGCAAGCGCCATGTGTAAGCCATC 3') and phosphorylated primer 310-30 (5' ATTCTCTTTTGAAGTATTGCTCCC 3'), using 100 ng of clone 4A1 as the template. PCR was carried out using 2.5 units of cloned pfu DNA polymerase (Stratagene, La Jolla, CA) with the buffer provided and 30 pmol of each primer. Thirty cycles of  $94^{\circ}\text{C}$  for 1 min,  $56^{\circ}\text{C}$  for 1 min, and  $72^{\circ}\text{C}$  for 2.5 min were carried out in a Perkin-Elmer Cetus (Norwalk, CT) DNA Thermocycler. The resulting 784 bp PCR product was purified on FMC (Rockland, ME) spinbind and ligated to 12.5 pmol of His-tag adaptor formed by annealing phosphorylated primer 310-31 (5' CACCACCATCATCACCCTAGC 3') and 310-032 (5' GGCCGCTAGTG-

GTGATGATGGTGGTG 3'). The ligated DNA was digested with the restriction endonuclease *NotI* and purified by electrophoresis in 1% low melting point agarose. The excised band was treated with  $\beta$ -agarase (FMC, Rockland, ME) and ligated to the vector pCH250, a derivative of pCDM8 (42), at the unique *NotI* site to produce plasmid pCH254. For expression in insect cells, plasmid pCH254 was digested with *NotI* and the 0.8 kb fragment containing the  $\gamma_{\text{His}}$  cDNA was recovered by FMC spinbind purification and ligated into *NotI* digested and phosphatase-treated pFastBac I (Life Technologies Inc., Gaithersburg, MD). Recombinant Bacmid DNA was prepared and transfected into *Spodoptera frugiperda* (Sf9) cells according to the manufacturer's recommendations. High titer baculovirus stocks were subsequently prepared by infection of Sf9 cells.

The protein was expressed in High-Five insect cells. A 36 L culture of cells grown to a density of  $2.1 \times 10^6$  cells/mL in Sf900 II medium at  $28^{\circ}\text{C}$  was infected with the pFastBac I baculovirus containing the  $\gamma_{\text{His}}$  cDNA at a MOI of 3.5 virions/cell. Fresh Sf900 II medium (2 L) was added at the time of infection, and the culture was harvested 44 h postinfection. Cells and debris were removed by filtration through 0.5 and 0.2  $\mu\text{m}$  filters connected in series, then sodium azide and the protease inhibitors AEBSF, benzamide, leupeptin, aprotinin, and pepstatin were added to final concentrations of 0.05%, 200  $\mu\text{M}$ , 1 mM, 10  $\mu\text{g/mL}$ , 10  $\mu\text{g/mL}$ , and 1  $\mu\text{g/mL}$ , respectively. The cell-free supernatant was then concentrated to 3 L by ultrafiltration with three S1Y10 spiral membrane cartridges (Amicon) connected in series. The concentrate was stored at  $-70^{\circ}\text{C}$ . Typically, the protein was purified from 800 mL of the concentrated medium by first dialyzing against 50 mM  $\text{Na}_2\text{HPO}_4$ , pH 8, 0.5 M NaCl, and 20 mM imidazole, centrifuging to remove insoluble material and then loading the supernatant onto a 45 mL (2.6 cm internal diameter  $\times$  8.5 cm) column of  $\text{Ni}^{2+}$ -NTA agarose equilibrated with 50 mM  $\text{Na}_2\text{HPO}_4$ , pH 8, 0.5 M NaCl, and 20 mM imidazole. Once loaded, the column was washed with 1050 mL of the equilibration buffer before the bound proteins were eluted with a linear 20 to 250 mM imidazole gradient (total volume = 500 mL) in 50 mM  $\text{Na}_2\text{HPO}_4$ , pH 8, and 0.5 M NaCl. Fractions identified as containing  $\gamma_{\text{His}}$  by reducing SDS-PAGE were pooled and dialyzed extensively against 40 mM  $\text{Na}_2\text{HPO}_4$ , pH 7.5. Highly aggregated forms of  $\gamma_{\text{His}}$  were then removed by gel filtration through two Superdex 200 HR 10/30 columns (Pharmacia) connected in series at 0.4 mL/min in either PBS or HEPES buffered saline (HBS),<sup>1</sup> depending on whether the protein was to be used for gel filtration or SPR experiments, respectively. The gel filtered  $\gamma_{\text{His}}$  was stored at 0.2 mg/mL in either buffer at  $-70^{\circ}\text{C}$ .

**Protein Concentration Determination.** The concentration of IL-2R $\beta$  was determined from absorbance measurements at 280 nm using a molar absorption coefficient of  $58\,200\text{ L mol}^{-1}\text{ cm}^{-1}$ , which was calculated from amino acid analysis data. The concentrations of  $\gamma_{\text{His}}$  and IL-2 were determined using the predicted molar absorption coefficients of  $61\,450\text{ L mol}^{-1}\text{ cm}^{-1}$  and  $9650\text{ L mol}^{-1}\text{ cm}^{-1}$ , respectively (43). For the various mAb and Fab fragments, extinction coefficients of  $214\,500\text{ L mol}^{-1}\text{ cm}^{-1}$  and  $76\,500\text{ L mol}^{-1}\text{ cm}^{-1}$ , respectively, were used (44).

**N-Terminal Sequencing.** The N-terminal sequence of IL-2R $\beta$  and  $\gamma_{\text{His}}$  were determined using a model 470A gas-phase

<sup>2</sup> Whitty, A., Raskin, N., Olson, D. L., Borysenko, C. W., Benjamin, C. D., and Burkly, L. C. (1998) Interaction affinity between cytokine receptor components on the cell surface (submitted for publication).



sequencer (Applied Biosystems, Foster City, CA). Protein (200 pmol) was loaded directly and the resulting PTH-amino acids were analyzed on-line using a model 120A amino acid analyzer (Applied Biosystems) fitted with a C<sub>18</sub> (2.1 mm internal diameter × 220 mm) reversed-phase HPLC column.

**Analysis of the Binding of IL-2 to COS-7 Cells Transfected with the cDNA Encoding the Full-Length IL-2R $\beta$  and  $\gamma_c$  Chains.** COS-7 cells ( $10^7$  in 0.8 mL of 20 mM HEPES, 0.7 mM Na<sub>2</sub>HPO<sub>4</sub>, pH 7.05, 137 mM NaCl, 5 mM KCl, and 6 mM dextrose) were transfected by electroporation with 20  $\mu$ g each of the derivatives of the pCDM8 (42) expression vector pLB009 and pLB026 which carry the full-length cDNA of the IL-2R $\beta$  and  $\gamma_c$  chains, respectively. Binding of [<sup>125</sup>I]IL-2 to the transfected cells was determined 48 h posttransfection. Cells ( $5 \times 10^6$ ) were preincubated in 150  $\mu$ L of PBS containing 1% fetal calf serum (FCS) for 1 h at 4 °C in the absence or presence of mAb CP.B8 or its Fab fragment or the murine IgG<sub>1</sub> isotype control MOPC 21 or its Fab fragment. [<sup>125</sup>I]IL-2 ( $2.1 \times 10^{16}$  Bq/mol) was then added to a concentration of 1 nM, and the cells were incubated for a further 1 h at 4 °C. The cells were then washed twice with 2 mL of PBS containing 1% FCS, and the amount of bound radioactivity was determined by counting in a Wallac (Gaithersburg, MD) 1470 gamma counter. The data were corrected for nonspecific IL-2 binding by deducting the amount of bound counts from a sample which contained 1 nM [<sup>125</sup>I]IL-2 and a 100-fold molar excess of nonradioactive IL-2.

**Gel Filtration Analysis of the Formation of the IL-2/IL-2R $\beta$ / $\gamma_{His}$  Complex.** To investigate the formation of the IL-2/IL-2R $\beta$ / $\gamma_{His}$  complex, 200 pmol (1.58  $\mu$ M) of IL-2, IL-2R $\beta$ ,  $\gamma_{His}$  monomer, or  $\gamma_{His}$  dimer, either alone or in combination, were incubated for 1 h at room temperature and then 158 pmol was removed and gel filtered through two Superdex 200 HR 10/30 columns connected in series at 0.4 mL/min in PBS. The effluent was monitored at 280 nm, and the columns were calibrated with gel filtration standards (Bio-Rad) containing BSA as an additional standard. Plots of elution time versus log  $M_r$  for the standards typically yielded straight lines with correlation coefficients of  $R^2 = 0.97-0.99$ . Fractions (500  $\mu$ L) were collected and the location of IL-2R $\beta$  determined by Western dot-blot analysis. Samples (50  $\mu$ L) of selected gel filtration fractions were applied under vacuum to 0.45  $\mu$ m nitrocellulose filters (Bio-Rad) in a 96-well dot-blot chamber (Bio-Rad). The loaded nitrocellulose was removed from the chamber and blocked overnight with 20 mM Tris-HCl, pH 7.2, 150 mM NaCl, 2% nonfat dry milk, and 0.05% sodium azide. To detect IL-2R $\beta$ , blots were incubated for 1 h in 20 mM Tris-HCl, pH 7.2, 150 mM NaCl, 2% nonfat dry milk, 0.5% Tween 20, and 0.05% sodium azide, containing 1  $\mu$ g/mL mAb 18741D. After washing the blots with 4 × 5 min washes of 20 mM Tris-HCl, pH 7.2, 150 mM NaCl, and 0.5% Tween 20 (buffer A), followed by 5 × 5 min washes with 20 mM Tris-HCl, pH 7.2, and 150 mM NaCl (buffer B), the bound mAb 18741D was detected by incubating the blots for 1 h in 20 mM Tris-HCl, pH 7.2, 150 mM NaCl, 2% nonfat dry milk, and 0.05% sodium azide, containing a 1:1000 dilution of HRP-conjugated goat anti-mouse IgG (Bio-Rad). After washing the blots with 5 × 5 min washes of buffer B followed by a final rinse with 10 mM Tris-HCl, pH 7.2, the blots were developed and visualized with ECL chemilumi-

nescent reagents (Amersham, Cleveland, OH) according to the manufacturer's instructions.

**Gel Filtration Analysis of the Interaction between MAb CP.B8 and  $\gamma_{His}$ .** For gel filtration experiments designed to investigate the interaction of mAb CP.B8 with  $\gamma_{His}$ , 115 pmol (0.77  $\mu$ M) of mAb CP.B8 or  $\gamma_{His}$  monomer, either alone or in combination, were incubated for 30 min at room temperature, and then 77 pmol were removed and gel filtered through two Superdex 200 HR 10/30 columns connected in series at 0.4 mL/min in PBS.

For gel filtration experiments designed to investigate the inhibition of formation of the IL-2/IL-2R $\beta$ / $\gamma_{His}$  complex by mAb CP.B8, 200 pmol of  $\gamma_{His}$  monomer and 1 nmol of mAb CP.B8 were incubated for 30 min at room temperature, and then 200 pmol of IL-2 and IL-2R $\beta$  were added. After a further 30 min incubation at room temperature, 158 pmol of IL-2, IL-2R $\beta$ , and  $\gamma_{His}$  monomer and 796 pmol of mAb CP.B8 were removed and gel filtered through two Superdex 200 HR 10/30 columns connected in series at 0.4 mL/min in PBS. In other experiments designed to investigate the ability of mAb CP.B8 to bind to  $\gamma_{His}$  monomer already complexed with IL-2 and IL-2R $\beta$ , 200 pmol of IL-2, IL-2R $\beta$ , and  $\gamma_{His}$  monomer were incubated for 30 min at room temperature, and then 1 nmol of mAb CP.B8 was added. After a further 30 min incubation at room temperature, 158 pmol of IL-2, IL-2R $\beta$ , and  $\gamma_{His}$  monomer and 796 pmol of mAb CP.B8 were removed and gel filtered as described above.

**Preparation of Protein Reagents for SPR.** Prior to SPR analysis, IL-2 was dialyzed extensively against HBS and centrifuged to remove insoluble material. The mAb CP.B8 and MOPC 21 were gel filtered through two Superdex 200 HR 10/30 columns connected in series at 0.4 mL/min in HBS to exact a buffer change and to remove aggregated material. The Fab fragments of CP.B8 and MOPC 21 were generated by digestion of the intact antibodies with immobilized papain in 20 mM Na<sub>2</sub>HPO<sub>4</sub>, pH 7, 10 mM EDTA, and 20 mM cysteine-HCl, at 37 °C for 6 h. The undigested antibody and the cleaved Fc fragment were removed by passing the sample over a column of Protein A Fast Flow resin (Pharmacia). The flow through, containing the Fab fragment, was dialyzed extensively against PBS, concentrated, and then the Fab fragment was purified further by gel filtration in HBS as described above. The fidelity of the Fab fragments was confirmed on calibrated reducing and nonreducing SDS-PAGE gels.

All protein reagents except IL-2R $\beta$  were formulated at the desired concentrations in HBS containing 0.005% surfactant P20 and 0.1 mg/mL BSA. BSA was included to reduce the bulk refractive index difference between the sample and the running buffer (45).

**SPR Analysis of the Formation of the IL-2/IL-2R $\beta$ / $\gamma_{His}$  Complex.** All SPR experiments were carried out using a BIAcore 2000 instrument (BIAcore Inc., Piscataway, NJ) at a flow rate of 10  $\mu$ L/min. Pure IL-2R $\beta$  was coupled covalently to the CM5 chip as follows. The CM5 chip surface was first activated with *N*-hydroxysuccinimide/*N*-ethyl-*N'*-(3-diethylaminopropyl)carbodiimide (15–30  $\mu$ L), and then IL-2R $\beta$  (20–50  $\mu$ L) diluted to 20–30  $\mu$ g/mL in 10 mM acetic acid, pH 4, was injected. Unreacted groups on the chip were then blocked with ethanolamine-HCl (30–35  $\mu$ L). In such a manner, surface densities of between 4457

and 6999 resonance units (RU) were generated. Following several rounds of regeneration with 1 mM formic acid (20  $\mu$ L) to establish a reproducible and stable baseline, samples of IL-2 and  $\gamma_{\text{His}}$  were injected over the surface, either alone or in combination, in HBS containing 0.005% P20 and 0.1 mg/mL BSA. Time courses ("sensorgrams") were recorded and normalized to a baseline of 0 RU, and equivalent volumes of all samples were run simultaneously over a blank, (i.e., nonprotein, blocked) surface to allow deduction of nonspecific, bulk refractive index changes (46). The surface was regenerated between samples by injecting 1 mM formic acid (20  $\mu$ L), followed by reequilibration with HBS containing 0.005% P20 and 0.1 mg/mL BSA. Data were analyzed using the BIAevaluation 2.1 software supplied with the instrument. Data for the binding of IL-2 alone to the chip showed, at high concentrations of IL-2, a slight drift of  $<0.022$  RU/s in the signal observed at equilibrium. The size of the burst in RU, corresponding to the equilibrium binding at each concentration of IL-2, was determined by a linear extrapolation of the data for  $t = 20$ –150 s back to  $t = 0$  (where  $t = 0$  is the injection time). This correction never exceeded 1% of the signal observed at  $t = 20$  s. Sensorgrams for the binding of  $\gamma_{\text{His}}$  to the chip in the presence of IL-2 showed an initial burst in RU followed by a slower phase of binding. Data for the slower phase deviated systematically from a single exponential, but an improved fit was obtained by allowing for a linear drift in the signal of 0.016 RU/s, similar in magnitude to that observed in data for the binding of IL-2 alone. This drift could not be eliminated by changing the experimental conditions, nor could the cause of this additional slow association be established, although it is likely to be due to the nonspecific binding of IL-2 and/or  $\gamma_{\text{His}}$  to the chip. For each combination of IL-2 and  $\gamma_{\text{His}}$  concentrations, the data from  $t = 10$ –600 s after injection were fitted to an exponential equation with allowance for drift, offset from 0 RU by an amount corresponding to the size of the initial burst. The size of the initial burst was given by the offset, and the amplitude of the slow phase of binding was determined from the exponential component of the fit.

For the inhibition of IL-2/IL-2R $\beta$ / $\gamma_{\text{His}}$  complex formation by either mAb CP.B8 or MOPC 21, or by their respective Fab fragments, the antibodies were preequilibrated with IL-2 and  $\gamma_{\text{His}}$  for 15 min prior to injection over the IL-2R $\beta$  surface.

## RESULTS

**MAb CP.B8 and Its Fab Fragment Inhibit the Formation of the Intermediate Affinity IL-2R on the Surface of Transfected COS-7 Cells.** MAb CP.B8, an antibody directed against the extracellular portion of the human  $\gamma_c$  chain, has been shown to inhibit the IL-2-dependent proliferation of freshly isolated human peripheral blood mononuclear cells (PBMC) when cultured with allogeneic targets, and to inhibit the IL-2-dependent proliferation of PHA-activated T cells by blocking the high-affinity binding ( $K_d = 10$  pM) of IL-2 to the IL-2R $\alpha$ /IL-2R $\beta$ / $\gamma_c$  complex (40). We carried out experiments to determine whether the antibody similarly inhibited binding of IL-2 to the intermediate affinity IL-2R, using, as a model system, COS-7 cells which were transfected with the cDNA for the full-length IL-2R $\beta$  and  $\gamma_c$  chains.

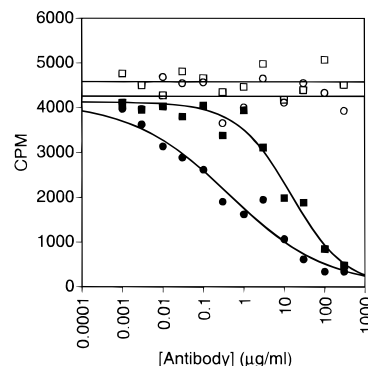


FIGURE 1: Inhibition of the binding of [ $^{125}$ I]IL-2 to COS-7 cells expressing the full-length IL-2R $\beta$  and  $\gamma_c$  chains by mAb CP.B8 and its Fab fragment. COS-7 cells transfected with cDNA encoding the full-length IL-2R $\beta$  and  $\gamma_c$  chains were incubated with various concentrations of mAb CP.B8 (●) or its Fab fragment (■), the murine IgG1 isotype control MOPC 21 (○), or its Fab fragment (□), and the amount of [ $^{125}$ I]IL-2 bound to the cells determined as described in the Experimental Procedures. The data for mAb CP.B8 and its Fab fragment were fitted to a four parameter curve fit with the maximum number of specific counts bound in the absence of antibody set at 4125 CPM as determined experimentally.

Figure 1 shows that both mAb CP.B8 and its Fab fragment specifically inhibited the binding of 1 nM [ $^{125}$ I]IL-2 to the surface of the transfected cells. This concentration of IL-2 was chosen since it equals the  $K_d$  for the binding of IL-2 to the IL-2R $\beta$ / $\gamma_c$  complex (26). At a concentration of 300  $\mu$ g/mL (2  $\mu$ M), mAb CP.B8 blocked 92% of IL-2 binding, while at 300  $\mu$ g/mL (6  $\mu$ M), its Fab fragment blocked 88% of binding. The  $IC_{50}$  values were 0.4  $\mu$ g/mL (2.7 nM) for the intact antibody and 15  $\mu$ g/mL (300 nM) for the Fab fragment. By contrast, neither the murine IgG1 isotype control MOPC 21 nor its Fab fragment yielded significant inhibition at these concentrations.

**Characterization of Recombinant Soluble  $\gamma_{\text{His}}$ .** The ability of mAb CP.B8 and its Fab fragment to inhibit the binding of IL-2 to the intermediate affinity IL-2R on the surface of transfected COS-7 cells suggested that it functioned by blocking a critical site on the  $\gamma_c$  chain required for interaction with IL-2 and/or IL-2R $\beta$ . To define this mechanism at the molecular level, we prepared the individual components and tested the ability of mAb CP.B8 to inhibit complex formation in solution.

Purification of  $\gamma_{\text{His}}$  on Ni $^{2+}$ -NTA agarose as described in the Experimental Procedures typically resulted in preparations which were  $>95\%$  homogeneous as judged by reducing SDS-PAGE. The N-terminal sequence, L(N)T(T)ILTP-NGNEDT(T)ADFFL, agreed with the published sequence (1), although Asn at position 2 and Thr at positions 4 and 15 could not be identified. The apparent  $M_r$  of  $\gamma_{\text{His}}$  on calibrated reducing SDS-PAGE gels ( $M_r = 49\,000 \pm 0$ ,  $n = 5$ ) was significantly greater than the predicted mass based on the amino acid composition alone ( $M_r = 28\,186$ ), indicating that at least some of the six predicted glycosylation sites (1) were occupied. Although  $\gamma_{\text{His}}$  ran as a single band on reducing SDS-PAGE, gel filtration through a Superose 6 HR 10/30 column indicated that, under native conditions, the protein formed two prominent species with apparent  $M_r$  values of 42 800 and  $1.2 \times 10^5$ , as well as more highly aggregated forms, the largest of which eluted close to the  $4 \times 10^7$   $M_r$  exclusion limit of the column. Therefore, it

appeared that  $\gamma_{\text{His}}$  existed primarily as monomeric and trimeric species. However, cross-linking with disuccinimidyl glutarate followed by reducing SDS-PAGE indicated that the cross-linked species was dimeric, with no evidence of a trimeric species (data not shown). While we cannot rule out the possibility that the oligomeric form is a trimer but fails to cross-link as such under the conditions used, our assignment of this species as a dimer is in agreement with Hoffman et al. (47, 48). The anomalous behavior of the dimeric form on gel filtration was presumably due to the highly glycosylated nature of the protein.

Initial SPR studies showed that the monomeric form of  $\gamma_{\text{His}}$  was able to associate with IL-2R $\beta$  in the presence of IL-2, but that the dimeric form was largely devoid of activity. Experiments to find conditions that would minimize the formation of dimer in the  $\gamma_{\text{His}}$  preparation showed that the most important factor affecting the relative amount of dimer was the protein concentration. If the concentration was maintained at 0.5 mg/mL or higher, the ratio of dimer to monomer typically ranged from 3:1 to 5:1 (w/w). However, by keeping the concentration at no more than 0.2 mg/mL, the ratio of dimer to monomer could be kept at approximately 1:1 (w/w). Attempts were made to separate completely the dimeric and monomeric forms by gel filtration through two Superdex 200 HR 10/30 columns connected in series. However, due to the propensity of  $\gamma_{\text{His}}$  to aggregate even after separating the two species and rechromatographing the isolated peaks one or two additional times, it was not possible to prepare monomeric  $\gamma_{\text{His}}$  uncontaminated by the dimeric form. For the gel filtration experiments, preparations which were enriched for the monomeric or dimeric forms of  $\gamma_{\text{His}}$  were used, while for the SPR experiments preparations containing both forms at a ratio of approximately 1:1 (w/w) were used.

During the course of the present study, we also expressed and purified the extracellular portion of the murine  $\gamma_c$  chain as a His-tagged construct, a protein which is 69% identical at the amino acid sequence level to the human protein (49). Interestingly, unlike the human protein, murine  $\gamma_{\text{His}}$  ran on gel filtration as a monomeric species with an apparent  $M_r$  of 49 600 even at a concentration of 0.91 mg/mL, a concentration at which most of the human  $\gamma_{\text{His}}$  is dimeric. The ability to purify monomeric murine  $\gamma_{\text{His}}$  may prove useful for X-ray crystallography studies aimed at determining the structure of the murine IL-2/IL-2R $\beta$ / $\gamma_c$  complex, or of other cytokine receptor complexes which utilize the  $\gamma_c$  chain.

**Detection of a Stable Complex between IL-2 and IL-2R $\beta$  by Gel Filtration Is Dependent upon  $\gamma_{\text{His}}$ .** To investigate the role of  $\gamma_{\text{His}}$  in the formation of the IL-2/IL-2R $\beta$ / $\gamma_{\text{His}}$  complex, a series of experiments was carried out in which IL-2, IL-2R $\beta$ , and  $\gamma_{\text{His}}$  were analyzed by gel filtration, both individually and as mixtures of two and three components. The formation of a stable complex was determined not only by comparison of the gel filtration chromatograms, but also by detecting the position of IL-2R $\beta$  in the elution profile and any shift in its position due to its inclusion in a higher  $M_r$  complex, by Western dot-blot analysis. Control samples which did not contain IL-2R $\beta$  were also subjected to Western dot-blot analysis to demonstrate that there was no nonspecific cross-reactivity of IL-2 or  $\gamma_{\text{His}}$  with mAb 18741D and HRP-conjugated goat anti-mouse IgG used to detect IL-2R $\beta$ .

When tested separately, IL-2 ran as a single peak with an apparent  $M_r$  of 12 200 (Figure 2A), while IL-2R $\beta$  ran as two peaks, a major peak with an apparent  $M_r$  of 30 300 corresponding to the monomer and a minor peak with an apparent  $M_r$  of 62 200, which was presumably a dimeric form (Figure 2B). The apparent  $M_r$  of monomeric IL-2R $\beta$  agreed well with the apparent  $M_r$  values of  $33\,400 \pm 550$  ( $n = 5$ ) and  $31\,000 \pm 670$  ( $n = 10$ ) determined on calibrated reducing and nonreducing SDS-PAGE gels, respectively. Preparations of  $\gamma_{\text{His}}$  that were enriched for the monomeric (Figure 2C) or dimeric (Figure 2D) forms (referred to hereafter as  $\gamma_{\text{His}}$  monomer and  $\gamma_{\text{His}}$  dimer, respectively) yielded apparent  $M_r$  values of 49 800 and 152 700, respectively. Western dot-blot analysis of the individual components indicated that only IL-2R $\beta$  was detected after incubation of the blots with mAb 18741D followed by HRP-conjugated goat anti-mouse IgG (Figure 3). The Western positive material eluted in fractions 34–36, which corresponded to the monomeric form of IL-2R $\beta$ . The dimeric form of IL-2R $\beta$  was not detected presumably because the epitope for mAb 18741D was masked by the dimerization.

When tested in pairs—IL-2 + IL-2R $\beta$  (Figure 2E), IL-2 +  $\gamma_{\text{His}}$  monomer (Figure 2F), IL-2R $\beta$  +  $\gamma_{\text{His}}$  monomer (Figure 2G), and IL-2R $\beta$  +  $\gamma_{\text{His}}$  dimer (Figure 2H)—there was no evidence for any stable complexes between the various proteins since the chromatograms were identical to the sum of their individual components. Furthermore, Western dot-blot analysis indicated that the position of IL-2R $\beta$  remained essentially unchanged in the presence of either IL-2,  $\gamma_{\text{His}}$  monomer, or  $\gamma_{\text{His}}$  dimer (Figure 3). However, a stable complex was formed when IL-2, IL-2R $\beta$ , and  $\gamma_{\text{His}}$  monomer were incubated and run as a mixture under the same conditions. As can be seen from Figure 2I, the size of the IL-2R $\beta$  peak was reduced significantly in the presence of IL-2 and  $\gamma_{\text{His}}$  monomer, and a new peak (marked with an asterisk), with an apparent  $M_r$  of 58 400, was formed. Moreover, Western dot-blot analysis clearly demonstrated that the position of IL-2R $\beta$  shifted to a higher  $M_r$  in the presence of IL-2 and  $\gamma_{\text{His}}$  monomer since the protein was detected in fractions 26–35 (Figure 3). Although the complex was larger than either IL-2, IL-2R $\beta$ , or  $\gamma_{\text{His}}$  monomer alone, the apparent  $M_r$  was significantly lower than the calculated mass (92 300) for a 1:1:1 stoichiometry of the three gel filtered components. However, neither the mixture containing IL-2 + IL-2R $\beta$  (Figure 2E) nor IL-2R $\beta$  +  $\gamma_{\text{His}}$  monomer (Figure 2G) resulted in a shift in the position of IL-2R $\beta$  to a higher  $M_r$ , indicating that the complex observed in Figure 2I and Figure 3 contained all three proteins.

We also tested the ability of dimeric  $\gamma_{\text{His}}$  to form a complex with IL-2R $\beta$  in the presence of IL-2. Unlike the monomeric form of  $\gamma_{\text{His}}$ , which promoted the inclusion of most of the IL-2R $\beta$  into a higher  $M_r$  complex (Figure 2I), dimeric  $\gamma_{\text{His}}$  shifted the position of only a small portion of IL-2R $\beta$ , leaving most of it unassociated (Figure 2J). Indeed, the presence of a complex in fractions 24–26 was not apparent from the chromatogram itself, but could be detected by the more sensitive Western dot-blot analysis (Figure 3). This result indicates that while most of dimeric  $\gamma_{\text{His}}$  is inactive, a small fraction of the population retains the ability to associate with IL-2 and IL-2R $\beta$ , presumably because the sites involved in binding to these proteins are not masked by the dimerization.



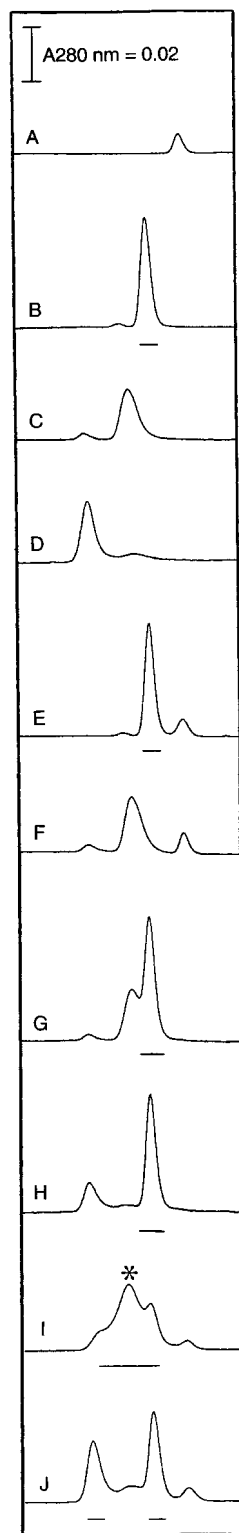


FIGURE 2: Gel filtration analysis of the formation of the IL-2/IL-2R $\beta$ / $\gamma$ <sub>His</sub> complex. IL-2, IL-2R $\beta$ ,  $\gamma$ <sub>His</sub> monomer, or  $\gamma$ <sub>His</sub> dimer (200 pmol, 1.58  $\mu$ M) were incubated, either alone or in combination, for 1 h at room temperature, and then 158 pmol was removed and gel filtered through two Superdex 200 HR 10/30 columns connected in series at 0.4 mL/min in PBS. The figure shows (A) IL-2, (B) IL-2R $\beta$ , (C)  $\gamma$ <sub>His</sub> monomer, (D)  $\gamma$ <sub>His</sub> dimer, (E) IL-2 + IL-2R $\beta$ , (F) IL-2 +  $\gamma$ <sub>His</sub> monomer, (G) IL-2R $\beta$  +  $\gamma$ <sub>His</sub> monomer, (H) IL-2R $\beta$  +  $\gamma$ <sub>His</sub> dimer, (I) IL-2 + IL-2R $\beta$  +  $\gamma$ <sub>His</sub> monomer, and (J) IL-2 + IL-2R $\beta$  +  $\gamma$ <sub>His</sub> dimer. The lines drawn underneath the chromatograms indicate the fractions containing IL-2R $\beta$  as determined by Western dot-blot analysis. The asterisk in chromatogram (I) marks the position of the peak corresponding to the IL-2/IL-2R $\beta$ / $\gamma$ <sub>His</sub> monomer complex.

The inability of the majority of dimeric  $\gamma$ <sub>His</sub> to form a complex with IL-2 and IL-2R $\beta$  confirmed our initial observations using SPR which showed that the dimeric form was largely inactive.

**MAb CP.B8 Blocks the Formation of the Stable IL-2/IL-2R $\beta$ / $\gamma$ <sub>His</sub> Complex.** Having established that a stable complex could be formed between IL-2, IL-2R $\beta$ , and  $\gamma$ <sub>His</sub> monomer, we proceeded to investigate the ability of mAb CP.B8 to form a complex with  $\gamma$ <sub>His</sub> and to determine the effect of such an association on the ability of  $\gamma$ <sub>His</sub> to interact with IL-2 and IL-2R $\beta$ . When tested alone, mAb CP.B8 ran as a single peak with an apparent  $M_r$  of 189 700 (Figure 4A), while monomeric  $\gamma$ <sub>His</sub> eluted with an apparent  $M_r$  of 48 000 (Figure 4B). For the mixture containing both mAb CP.B8 and  $\gamma$ <sub>His</sub>, two peaks eluted (Figure 4C), one which corresponded to the free antibody, and a larger peak with an apparent  $M_r$  of 402 000 (marked with an asterisk) which corresponded to a complex of the two proteins.

We next tested the ability of mAb CP.B8 to inhibit the formation of the IL-2/IL-2R $\beta$ / $\gamma$ <sub>His</sub> complex. When mAb CP.B8 and  $\gamma$ <sub>His</sub> were incubated prior to the addition of IL-2 and IL-2R $\beta$ , a peak consistent with the complex between mAb CP.B8 and  $\gamma$ <sub>His</sub> was detected (Figure 4D, marked with an asterisk). Moreover, the size of the IL-2R $\beta$  peak was essentially unchanged in the presence of the antibody (see Figure 2B for comparison), indicating that IL-2R $\beta$  was unable to associate with IL-2 and  $\gamma$ <sub>His</sub>. Similar results were also obtained when mAb CP.B8 was added after preincubation of IL-2, IL-2R $\beta$ , and  $\gamma$ <sub>His</sub> (Figure 4E), indicating that the antibody could dissociate  $\gamma$ <sub>His</sub> from the preformed IL-2/IL-2R $\beta$ / $\gamma$ <sub>His</sub> complex.

To understand further the molecular mechanisms underlying the association of IL-2, IL-2R $\beta$ , and  $\gamma$ <sub>His</sub> and the inhibition of complex formation by mAb CP.B8 and to obtain kinetic and equilibrium data for these processes, we carried out additional studies using SPR.

**SPR Analysis of the Formation of the IL-2/IL-2R $\beta$ / $\gamma$ <sub>His</sub> Complex.** Experiments were performed to study the binding of IL-2 and  $\gamma$ <sub>His</sub> to a BIAcore chip surface to which IL-2R $\beta$  had been coupled covalently, as described in the Experimental Procedures. Figure 5 shows data for the binding of IL-2 to the immobilized IL-2R $\beta$ . Examination of the individual sensorgrams (Figure 5, inset) showed that the association and dissociation of IL-2 are very fast; both processes are essentially complete within the dead time of the instrument ( $k_{\text{ass}} \geq 10^6 \text{ M}^{-1} \text{ s}^{-1}$ ,  $k_{\text{diss}} \geq 0.8 \text{ s}^{-1}$ ). Binding at equilibrium showed a hyperbolic dependence on IL-2 concentration, indicating that the IL-2R $\beta$  molecules on the chip surface constitute an apparently homogeneous population of binding sites for IL-2. The binding affinity,  $K_d = 800 \text{ nM} \pm 100 \text{ nM}$ , was in good agreement with published values (45). Figure 6 shows sensorgrams for the binding of 25  $\mu\text{g/mL}$  (890 nM)  $\gamma$ <sub>His</sub> to the IL-2R $\beta$ -derivatized chip in the presence of various concentrations of IL-2 from 14 to 3300 nM. Inclusion of  $\gamma$ <sub>His</sub> resulted in apparently biphasic progress curves for both the association and dissociation phases of binding, similar to that reported by Johnson et al. (50). The association phase is described by an initial burst of binding that is complete within the dead time of the instrument and which increases in magnitude with increasing IL-2 concentration, followed by a slower phase of binding that is not seen in the absence of  $\gamma$ <sub>His</sub> (Figure 5, inset). No

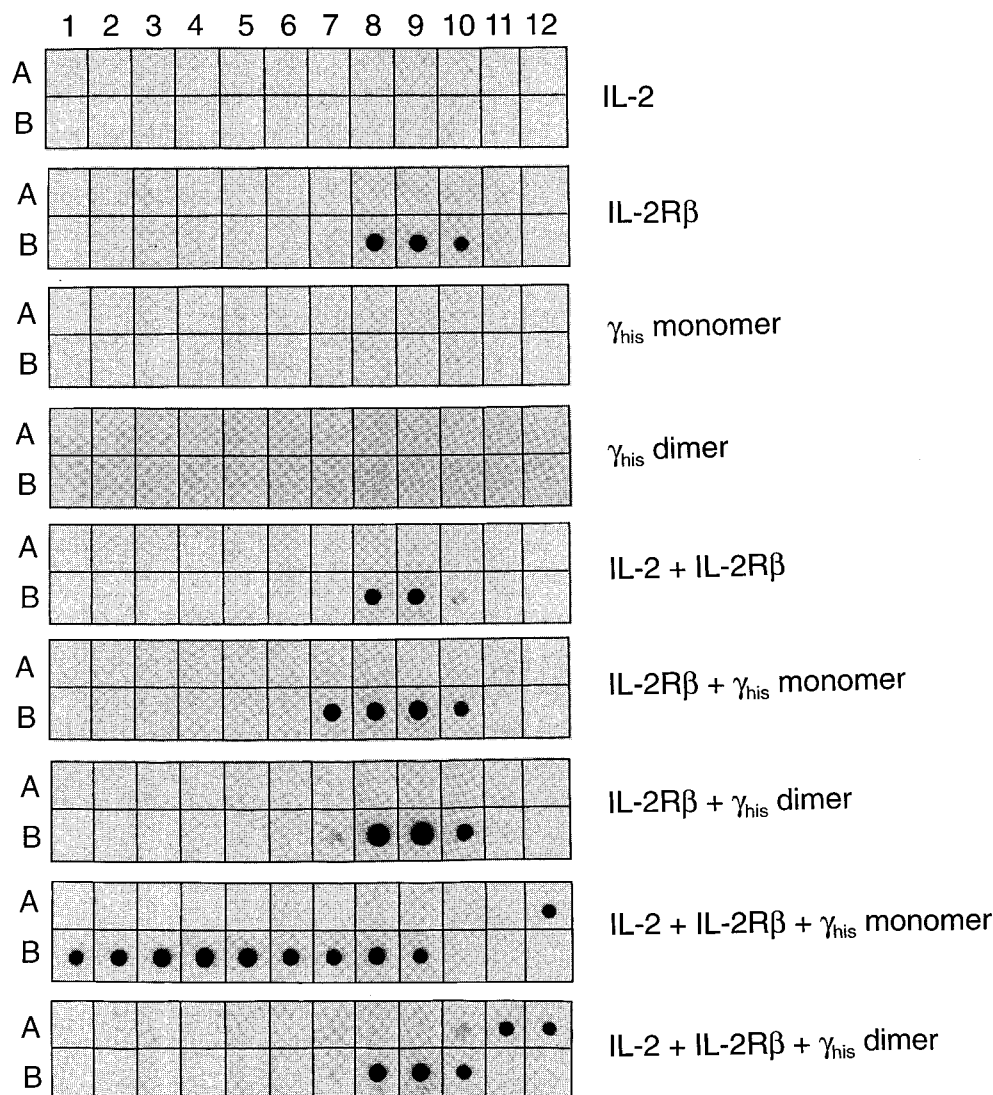


FIGURE 3: Western dot-blot analysis of the formation of the IL-2/IL-2R $\beta$ / $\gamma$ <sub>His</sub> complex. Samples (50  $\mu$ L) of fractions 15–38 from the gel filtration runs shown in Figure 2 were applied under vacuum to 0.45  $\mu$ m nitrocellulose filters in a 96-well dot-blot chamber and the position of IL-2R $\beta$  detected as described in the Experimental Procedures. The figure shows the scanned images of the dot-blot with a grid overlaid for clarity. From left to right: wells A1–A12 = fractions 15–26, and wells B1–B12 = fractions 27–38. Fractions from the gel filtration run containing IL-2 +  $\gamma$ <sub>His</sub> monomer (see Figure 2F) were not analyzed by Western dot-blot since neither protein was detected when run individually.

binding of  $\gamma$ <sub>His</sub> to the chip was seen in the absence of IL-2 (data not shown).

A more detailed analysis using various fixed concentrations of  $\gamma$ <sub>His</sub> from 110 to 3550 nM was performed. For each combination of IL-2 and  $\gamma$ <sub>His</sub> concentrations, the size of the initial burst was determined by taking data from  $t = 10$ –600 s and extrapolating it back to the injection time, as described in the Experimental Procedures. This showed that the magnitude of the initial burst was independent of the  $\gamma$ <sub>His</sub> concentration and, for a given IL-2 concentration, was comparable to the rapid binding seen in the absence of  $\gamma$ <sub>His</sub> (Figure 5, inset). This result suggested that the initial burst was due to the rapid binding of IL-2 to free IL-2R $\beta$  sites on the chip and showed this process to be unaffected by the presence of  $\gamma$ <sub>His</sub>. The gel filtration experiments described above established that IL-2 and  $\gamma$ <sub>His</sub> do not interact detectably in solution under these conditions. The  $\gamma$ <sub>His</sub>-dependent slow phase of binding was therefore interpreted to represent the slow association of  $\gamma$ <sub>His</sub> to the chip surface after the rapid equilibration with IL-2. In support of this conclusion, the

amplitude of the slow phase of binding, estimated as described in the Experimental Procedures, was observed to increase with increasing IL-2 concentration (Figure 6), as expected if  $\gamma$ <sub>His</sub> is binding to IL-2R $\beta$  sites that are already occupied by IL-2. Moreover, the concentration of IL-2 required to achieve maximal complex formation decreased with increasing  $\gamma$ <sub>His</sub> concentration and vice versa. This reciprocal interdependence supports the conclusion that the slow phase of binding represents the formation of an IL-2/IL-2R $\beta$ / $\gamma$ <sub>His</sub> complex on the chip. The maximum amplitude of the slow phase of binding, extrapolated to saturating concentrations of IL-2 and  $\gamma$ <sub>His</sub>, was only about half that expected from the maximum RU observed for the binding of IL-2 alone, suggesting that only about half of the sites that could bind IL-2 were capable of subsequently binding  $\gamma$ <sub>His</sub>. Although the several complicating features of the SPR data precluded a more detailed analysis of the binding kinetics, taken together the results show that IL-2 and  $\gamma$ <sub>His</sub> bind to IL-2R $\beta$  on a BIAcore chip surface to form a complex



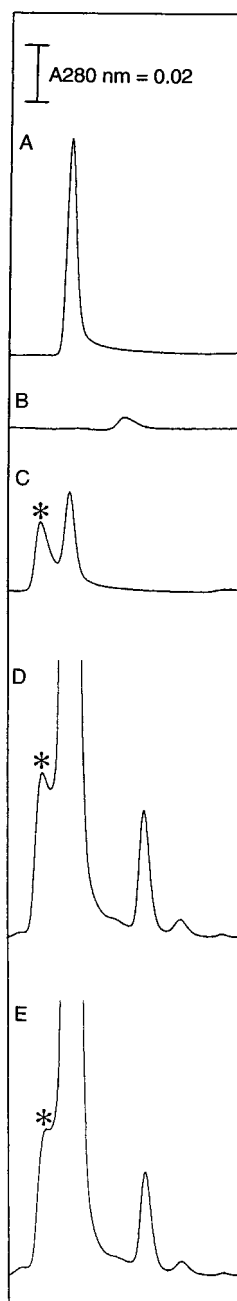


FIGURE 4: Gel filtration analysis of the association of mAb CP.B8 and  $\gamma_{\text{His}}$  monomer. For the association of mAb CP.B8 and  $\gamma_{\text{His}}$  monomer, 115 pmol (0.77  $\mu\text{M}$ ) of mAb CP.B8 (A),  $\gamma_{\text{His}}$  (B), or both mAb CP.B8 and  $\gamma_{\text{His}}$  (C) were incubated for 30 min at room temperature and then 77 pmol were removed and gel filtered through two Superdex 200 HR 10/30 columns connected in series at 0.4 mL/min in PBS. For the inhibition of formation of the IL-2/IL-2R $\beta$ / $\gamma_{\text{His}}$  complex by mAb CP.B8, (D) 1 nmol of mAb CP.B8 was mixed with 200 pmol of  $\gamma_{\text{His}}$  and incubated for 30 min at room temperature prior to the addition of 200 pmol of IL-2 and IL-2R $\beta$ . After a further 30 min incubation at room temperature, 158 pmol of IL-2, IL-2R $\beta$ , and  $\gamma_{\text{His}}$  and 796 pmol of mAb CP.B8 were removed and gel filtered as described above; (E) 200 pmol of IL-2, IL-2R $\beta$ , and  $\gamma_{\text{His}}$  were mixed and incubated for 30 min at room temperature prior to the addition of 1 nmol of mAb CP.B8. After a further 30 min incubation at room temperature, 158 pmol of IL-2, IL-2R $\beta$ , and  $\gamma_{\text{His}}$  and 796 pmol of mAb CP.B8 were removed and gel filtered as described above. The asterisks in chromatograms C, D, and E mark the position of the peak corresponding to the mAb CP.B8/ $\gamma_{\text{His}}$  complex.

that contains all three components and that this occurs through the initial rapid association of IL-2 to the im-

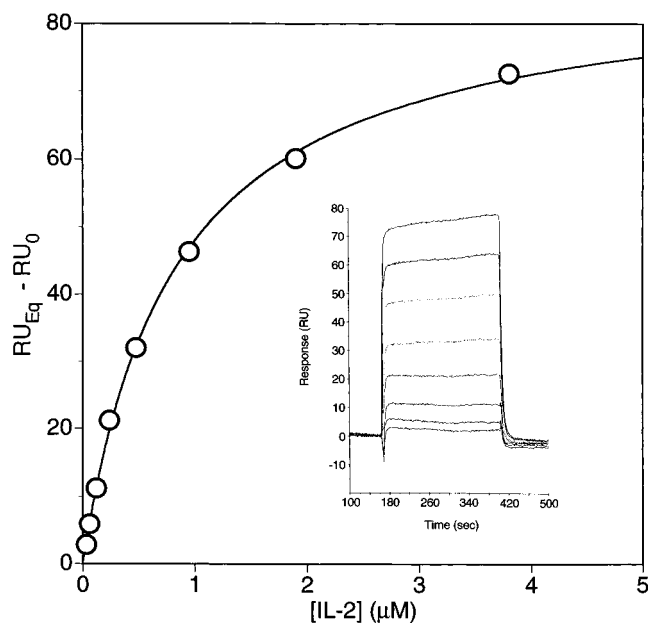


FIGURE 5: SPR analysis of the binding of IL-2 to immobilized IL-2R $\beta$ . IL-2 in HBS containing 0.005% P20 and 0.1 mg/mL BSA was injected at 10  $\mu\text{L}/\text{min}$  over a chip derivatized with 5307 RU of covalently coupled IL-2R $\beta$ . The main figure shows the measured RU (after background subtraction) at equilibrium as a function of the IL-2 concentration. The inset shows the sensorgrams (relative response in RU after background subtraction versus time) for IL-2 from 30 to 3800 nM (lower to upper curve: 30, 59, 119, 238, 475, 950, 1900, and 3800 nM IL-2).

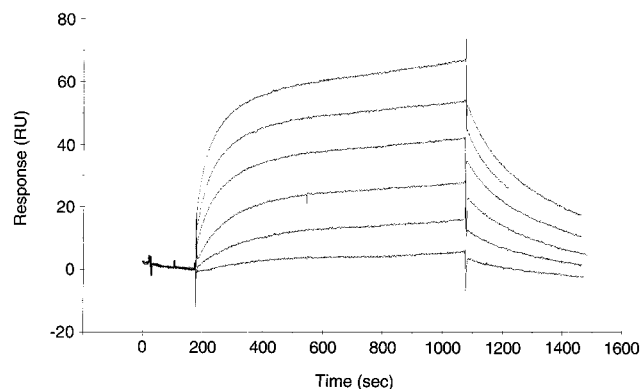


FIGURE 6: SPR analysis of the binding of IL-2 and  $\gamma_{\text{His}}$  to immobilized IL-2R $\beta$ . Samples of HBS containing 0.005% P20, 0.1 mg/mL BSA,  $\gamma_{\text{His}}$  (890 nM), and various concentrations of IL-2 were injected at 10  $\mu\text{L}/\text{min}$  over a chip derivatized with 6999 RU of covalently coupled IL-2R $\beta$ . The figure shows sensorgrams (relative response in RU after background subtraction versus time) for IL-2 from 14 to 3300 nM (lower to upper curve: 14, 41, 122, 367, 1100, and 3300 nM IL-2).

mobilized IL-2R $\beta$ , followed by the subsequent slow association of  $\gamma_{\text{His}}$ .

**MAb CP.B8 Blocks the Second Step in the Formation of the IL-2/IL-2R $\beta$ / $\gamma_{\text{His}}$  Complex.** The effect of mAb CP.B8 on the formation of the IL-2/IL-2R $\beta$ / $\gamma_{\text{His}}$  complex on the IL-2R $\beta$ -derivatized BIAcore chip was assessed by monitoring the binding of a fixed concentration of  $\gamma_{\text{His}}$  (6.25  $\mu\text{g}/\text{mL}$ , 220 nM) to the chip in the presence of 2080 nM IL-2 and 0–15  $\mu\text{g}/\text{mL}$  (0–100 nM) mAb CP.B8. Control experiments were run in the presence of the isotype control MOPC 21, to provide an estimate of any nonspecific effects of murine IgG<sub>1</sub> on binding. Figure 7A shows that mAb CP.B8 has no effect on the initial rapid association of IL-2 to IL-

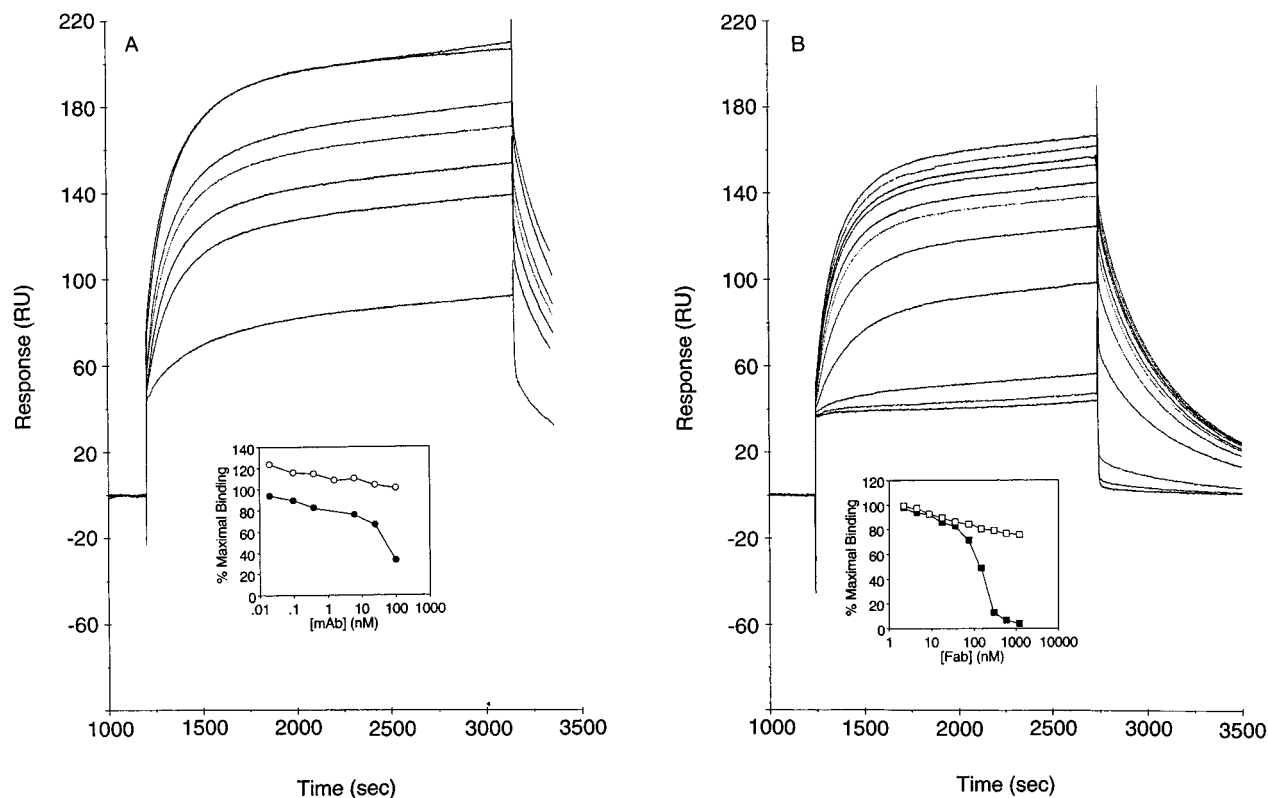


FIGURE 7: SPR analysis of the inhibition of  $\gamma_{\text{His}}$  binding to immobilized IL-2R $\beta$  in the presence of IL-2 by mAb CP.B8, MOPC 21, and their respective Fab fragments. (A) Samples of HBS containing 0.005% P20, 0.1 mg/mL BSA, IL-2 (2080 nM),  $\gamma_{\text{His}}$  (220 nM), and various concentrations of mAb CP.B8 or MOPC 21 were injected at 10  $\mu\text{L}/\text{min}$  over a chip derivatized with 5674 RU of covalently coupled IL-2R $\beta$ . The main figure shows sensorgrams (relative response in RU after background subtraction versus time) for mAb CP.B8 from 0 to 100 nM (upper to lower curve: 0, 0.02, 0.10, 0.39, 6.25, 25, and 100 nM mAb CP.B8). The inset shows the % maximal  $\gamma_{\text{His}}$ -dependent binding, relative to the binding in the absence of mAb, for MOPC 21 ( $\circ$ ) and mAb CP.B8 ( $\bullet$ ). (B) Samples of HBS containing 0.005% P20, 0.1 mg/mL BSA, IL-2 (2080 nM),  $\gamma_{\text{His}}$  (220 nM), and various concentrations of CP.B8 Fab or MOPC 21 Fab were injected at 10  $\mu\text{L}/\text{min}$  over a chip derivatized with 4457 RU of covalently coupled IL-2R $\beta$ . The main figure shows sensorgrams (relative response in RU after background subtraction versus time) for CP.B8 Fab from 0 to 1200 nM (upper to lower curve: 0, 2.3, 4.7, 9.4, 18.8, 37.5, 75, 150, 300, 600, and 1200 nM CP.B8 Fab). The inset shows the % maximal  $\gamma_{\text{His}}$ -dependent binding, relative to the binding in the absence of Fab, for MOPC 21 Fab ( $\square$ ) and CP.B8 Fab ( $\blacksquare$ ). Representative results from one of two independent experiments are shown.

2R $\beta$ , but that increasing concentrations of the antibody inhibit the subsequent slow phase of binding. This result indicates that the antibody blocks the association of  $\gamma_{\text{His}}$  to the IL-2/IL-2R $\beta$  complex. The inset plot in Figure 7A shows that inhibition of complex formation by mAb CP.B8 is dose dependent, and at concentrations above 10 nM the inhibition exceeds the small, nonspecific, effect seen with the control MOPC 21. The concentration of mAb CP.B8 required to inhibit binding of  $\gamma_{\text{His}}$  to the IL-2/IL-2R $\beta$  complex by 50% (i.e., the  $\text{IC}_{50}$  for mAb CP.B8) is between 25 nM and 100 nM. However, this value is comparable to the concentration of  $\gamma_{\text{His}}$  (220 nM) present in the experiment, and therefore it can be interpreted only as an upper limit to the potency with which mAb CP.B8 inhibits complex formation on the chip. Attempts to refine this limit by working at lower  $\gamma_{\text{His}}$  concentrations were unsuccessful due to the resulting decrease in the amplitude of the BIAcore response to levels at which accurate data could not be obtained. Figure 7B shows data from a similar experiment to that shown in Figure 7A with the same concentrations of IL-2 and  $\gamma_{\text{His}}$ , but using the Fab fragment of CP.B8 (0–60  $\mu\text{g}/\text{mL}$ , 0–1200 nM) rather than the intact mAb. Like the intact mAb, CP.B8 Fab blocked the slow second phase of binding in a dose-dependent fashion, while having no effect on the fast initial association of IL-2 to IL-2R $\beta$ . The inset plot in Figure 7B

shows that inhibition of complex formation by CP.B8 Fab is dose dependent, with an  $\text{IC}_{50} \approx 150$  nM, and exceeds the small, nonspecific, effect seen with MOPC 21 Fab.

## DISCUSSION

The experiments described in this report address the mechanism of action of mAb CP.B8, an antibody directed against the extracellular portion of the human  $\gamma_c$  chain, which blocks the binding of IL-2 to the intermediate affinity IL-2R expressed on the cell surface. Gel filtration and SPR analysis were used to establish the ability of components of the IL-2R to form a ternary complex in solution. Using gel filtration, we demonstrate that the formation of this complex is inhibited by mAb CP.B8. Using SPR analysis, we show that both the intact antibody and its Fab fragment block the recruitment of the  $\gamma_c$  chain into a complex with preformed IL-2/IL-2R $\beta$ .

Gel filtration analysis indicated that IL-2 did not form a stable complex with either IL-2R $\beta$  (Figure 2E and Figure 3) or with  $\gamma_{\text{His}}$  monomer (Figure 2F and Figure 3) and that IL-2R $\beta$  did not associate with  $\gamma_{\text{His}}$  monomer (Figure 2G and Figure 3), when the components were mixed in pairs at equal concentrations of 1.58  $\mu\text{M}$ . Incubation of all three proteins resulted in the formation of a stable complex with an apparent  $M_r$  of 58 400 (Figure 2I and Figure 3). Although the shift

in the position of IL-2R $\beta$  in the presence of IL-2 was dependent upon  $\gamma_{\text{His}}$  monomer, the apparent  $M_r$  of the complex was significantly lower than the calculated mass (92 300) for a 1:1:1 stoichiometry of the three gel filtered components. This anomalous behavior appears to be  $\gamma_{\text{His}}$ -dependent since the complex formed between IL-2 and IL-2R $\beta$  has been reported to have an apparent mass which is consistent with the sum of its two individual components (39). Similarly, in a gel filtration analysis of the association of  $\gamma_{\text{His}}$  with IL-4 and the IL-4R $\alpha$  chain (47, 48), the IL-4/IL-4R $\alpha$ / $\gamma_{\text{His}}$  monomer complex had an apparent  $M_r$  of 72 300, some 26 100 mass units lower than the calculated mass (98 400) for a 1:1:1 stoichiometry of the three components. By contrast, the IL-4/IL-4R $\alpha$  complex had an apparent  $M_r$  of 50 600, close to the sum of its two individual components (51 800). Although the reason for this discrepancy is not clear, it is possible that the protein(s) undergo conformational changes upon complex formation, becoming more compact and thereby lowering the apparent  $M_r$  of the complex or, alternatively, association of the glycosylated  $\gamma_{\text{His}}$  chain with IL-2 and IL-2R $\beta$  results in the sugar chains becoming less extended which would also lower the apparent  $M_r$ . Experiments using a deglycosylated  $\gamma_{\text{His}}$  chain would be required to address this question. Nevertheless, the fact that the apparent  $M_r$  of the IL-2/IL-2R $\beta$ / $\gamma_{\text{His}}$  complex was not larger than the calculated mass and that its behavior on gel filtration was strikingly similar to the IL-4/IL-4R $\alpha$ / $\gamma_{\text{His}}$  complex for which a 1:1:1 stoichiometry has been established (47, 48) is consistent with a 1:1:1 stoichiometry for the IL-2/IL-2R $\beta$ / $\gamma_{\text{His}}$  complex.

Gel filtration analysis established that a stable complex forms between IL-2, IL-2R $\beta$ , and  $\gamma_{\text{His}}$ , although the results cannot be interpreted with reference to the order in which the components associate since no complex was detected between any two of the three proteins tested. However, it is clear from the SPR analysis that the components of the intermediate affinity IL-2R associate in a sequential manner, with IL-2 binding first to IL-2R $\beta$ , to which  $\gamma_{\text{His}}$  then binds in a subsequent step. The binding of IL-2 to the immobilized IL-2R $\beta$  was fast ( $k_{\text{ass}} \geq 10^6 \text{ M}^{-1} \text{ s}^{-1}$ ) and led to the formation of a complex which dissociated rapidly ( $k_{\text{diss}} \geq 0.8 \text{ s}^{-1}$ ) when the IL-2 was no longer applied. The estimated limits to the association and dissociation rate constants are consistent with the values of  $k_{\text{ass}} = 1.27 \times 10^6 \text{ M}^{-1} \text{ s}^{-1}$  and  $k_{\text{diss}} = 0.66 \text{ s}^{-1}$  reported previously by Myszkowski et al. (45) using the same IL-2 as was used here but using a thiol-linked form of IL-2R $\beta$  in which the protein is tethered in a uniform manner to the chip surface. Similarly, the dissociation constant ( $K_d = 800 \text{ nM}$ ) determined from equilibrium binding measurements is less than 2-fold greater than the value of 480 nM obtained using the thiol-linked form of IL-2R $\beta$  (45). In our experiments, inclusion of  $\gamma_{\text{His}}$  resulted in biphasic curves for both the association and dissociation phases of binding (Figure 6). Although rate constants for these events could not be determined due to the unavoidable contamination of monomeric  $\gamma_{\text{His}}$  by the dimeric form, it is apparent that the  $\gamma_c$  chain slows the dissociation of the complex as compared to the very rapid dissociation of IL-2 from IL-2R $\beta$  (Figure 5, inset, and Figure 6). If the behavior of the isolated extracellular portion of the  $\gamma_c$  chain is representative of its behavior when part of the full-length protein expressed on the cell surface, then the effect of IL-2 would be to promote

the association of the extracellular portions of the IL-2R $\beta$  and  $\gamma_c$  chains, and thereby their cytoplasmic portions, by stabilizing the complex and reducing its dissociation. This interpretation is consistent with recent fluorescence resonance energy transfer studies which show that IL-2 induces a significant increase in the proximity of the IL-2R $\beta$  and  $\gamma_c$  chains on the surface of T cells (51). The IL-2/IL-2R $\beta$ / $\gamma_c$  chain complex that forms in solution, which can be analyzed by gel filtration and SPR, therefore provides a model for the intermediate affinity form of the IL-2R that is functional on resting T cells (31, 52), NK cells (32, 33), and on certain intestinal epithelial cells (13).

The ability to monitor the formation of the IL-2/IL-2R $\beta$ / $\gamma_{\text{His}}$  complex by gel filtration and SPR has enabled us to use this model system to test potential antagonists that will inhibit the recruitment of the  $\gamma_c$  chain into the complex. Gel filtration analysis indicates that mAb CP.B8 inhibits the formation of the IL-2/IL-2R $\beta$ / $\gamma_{\text{His}}$  complex by binding to and sequestering  $\gamma_{\text{His}}$ , thus preventing it from associating with IL-2 and IL-2R $\beta$  (Figure 4). Moreover, SPR analysis clearly demonstrated that both the intact antibody and its Fab fragment act by preventing the association of  $\gamma_{\text{His}}$  with the IL-2/IL-2R $\beta$  complex (Figure 7). This suggests that the binding site for the antibody on the  $\gamma_c$  chain is close to or within the contact interface that forms when  $\gamma_{\text{His}}$  binds to the IL-2/IL-2R $\beta$  complex. While our results do not rule out the possibility that mAb CP.B8 or its Fab fragment bind to a site distal from the contact interface and elicit a conformational change such that  $\gamma_{\text{His}}$  can no longer associate with the IL-2/IL-2R $\beta$  complex, our results are consistent with a recent epitope mapping study of the  $\gamma_c$  chain (40), which indicates that mAb CP.B8 binds to the  $\gamma_c$  chain at the junction of the two fibronectin type III-like domains.

SPR analysis of the inhibition of complex formation by the Fab fragment of CP.B8 also indicates that the antibody functions in a noncompetitive manner with respect to cytokine binding. As can be seen from Figure 7B, the sensorgram response does not diminish to zero even in the presence of saturating concentrations of the antibody; rather it plateaus at approximately 40 RU at  $\geq 600 \text{ nM}$  Fab once all of the  $\gamma_{\text{His}}$ -dependent binding has been inhibited. This residual response represents the binding of IL-2 to IL-2R $\beta$ , which is unaffected by the presence of the antibody and which cannot be reduced by increasing further the Fab concentration. Similarly, Whitty et al.<sup>2</sup> have shown that binding of intact mAb CP.B8 to the full-length  $\gamma_c$  chain expressed on the cell surface does not reduce binding of IL-4 to the IL-4R $\alpha$  chain, but rather prevents the subsequent association of the  $\gamma_c$  chain with the preformed IL-4/IL-4R $\alpha$  complex. Together, these results indicate that mAb CP.B8 functions to inhibit  $\gamma_c$  chain-dependent cytokine receptor formation and signaling by a common inhibitory mechanism in which the recruitment of the  $\gamma_c$  chain is blocked. In support of this notion, it has been shown that mAb CP.B8 inhibits the proliferative response of PHA-activated T cell blasts to IL-2, IL-4, and IL-15, as well as the IL-7 induced proliferation of freshly isolated human PBMC (40).

The ability to block the recruitment of the  $\gamma_c$  chain into the receptors for IL-2, IL-4, IL-7, and IL-15 raises the possibility of simultaneous inhibition of these and presumably also the IL-9R in pathological conditions such as systemic lupus erythematosus, rheumatoid arthritis, insulin-



dependent diabetes melitus, and Crohn's disease, where modulation of the immune system would be clinically desirable. Similarly, suppression of the immune system to prevent graft rejection after transplantation might be accomplished by inhibiting all of the  $\gamma_c$  chain-dependent cytokine receptors. It is well established that rejection of islet allografts in mice is mediated by infiltrating host cytotoxic T lymphocytes (CTL), activation and proliferation of which is driven by IL-2 (53, 54). However, in IL-2 (—/—) knockout mice, which still reject the transplanted allograft, it has been shown that intragraft expression of IL-4 and IL-7 (55) and of IL-15 (56) may mediate the activation of the infiltrating CTL in the absence of endogenous IL-2. Although antibodies directed against the IL-2R $\alpha$  chain, for example, have received considerable attention as immunosuppressants (35), such antagonists are limited by their need to compete with the cytokine for binding to the receptor specific chain. Furthermore, they inhibit only one cytokine receptor interaction leaving the other  $\gamma_c$  chain-dependent receptors unaffected. In circumstances such as those described above, blocking the recruitment of the  $\gamma_c$  chain into all of the  $\gamma_c$  chain-dependent cytokine receptors may be a better approach to immunosuppression than inhibition of a single cytokine receptor.

In summary, we have provided evidence that mAb CP.B8 inhibits the formation of the intermediate affinity IL-2R by preventing the recruitment of the  $\gamma_c$  chain into the receptor complex. This mechanism of inhibition is likely to extend to other cytokine receptors that employ the  $\gamma_c$  chain, offering a powerful approach to the modulation of immune responses in pathological settings and after organ transplantation.

## ACKNOWLEDGMENT

We thank Mark Krivopal for cloning the human  $\gamma_c$  chain gene, Dr. Christine Ambrose for cloning the murine  $\gamma_c$  chain gene, Richard Tizard, Janice Nelson, Christopher Tonkin, Michele McAuliffe, and Lars Tragethon for sequencing DNA, and Jennifer Kuesters for technical assistance. We also thank Dr. Thomas Ciardelli for supplying recombinant human IL-2 and the derivative of the pBlueBac II baculovirus expression vector encoding the IL-2R $\beta$  cDNA, and Dr. Zining Wu for performing preliminary SPR experiments.

## REFERENCES

1. Takeshita, T., Asao, H., Ohtani, K., Ishii, N., Kumaki, S., Tanaka, N., Munakata, H., Nakamura, M., and Sugamura, K. (1992) *Science* 257, 379–382.
2. Kondo, M., Takeshita, T., Ishii, N., Nakamura, M., Watanabe, S., Arai, K. I., and Sugamura, K. (1993) *Science* 262, 1874–1877.
3. Russell, S. M., Keegan, A. D., Harada, N., Nakamura, Y., Noguchi, M., Leland, P., Friedman, M. C., Miyajima, A., Puri, R. K., Paul, W. E., and Leonard, W. J. (1993) *Science* 262, 1880–1883.
4. Noguchi, M., Nakamura, Y., Russell, S. M., Ziegler, S. F., Tsang, M., Cao, X., and Leonard, W. J. (1993) *Science* 262, 1877–1880.
5. Russell, S. M., Johnston, J. A., Noguchi, M., Kawamura, M., Bacon, C. M., Friedmann, M., Berg, M., McVicar, D. W., Witthuhn, B. A., Silvennoinen, O., Goldman, A. S., Schmalsteig, F. C., Ihle, J. N., O'Shea, J. J., and Leonard, W. J. (1994) *Science* 266, 1042–1045.
6. Giri, J. G., Ahdieh, M., Eisenman, J., Shanenbeck, K., Grabstein, K., Kumaki, S., Namen, A., Park, L. S., Cosman, D., and Anderson, D. (1994) *EMBO J.* 13, 2822–2830.
7. Ishii, N., Takeshita, T., Kimura, Y., Tada, K., Kondo, M., Nakamura, M., and Sugamura, K. (1994) *Int. Immunol.* 6, 1273–1277.
8. Nakari, T., Robertson, M. J., Streuli, M., Wu, Z., Ciardelli, T. L., Smith, K. A., and Ritz, J. (1994) *J. Exp. Med.* 180, 241–251.
9. Bani, L., David, D., Moreau, J.-L., Cayota, A., Nakarai, T., Ritz, J., and Theze, J. (1997) *Int. Immunol.* 9, 573–580.
10. Schumann, R. R., Nakari, T., Gruss, H.-J., Brach, M. A., Von Arnim, U., Kirshning, C., Karawajew, L., Ludwig, W.-D., Renauld, J.-C., Ritz, J., and Herrmann, F. (1996) *Blood* 87, 2419–2427.
11. Itano, M., Tsuchiya, S., Morita, S., Fujie, H., Ishii, N., Yanagisawa, T., Ohashi, Y., Minegishi, M., Sugamura, K., and Konno, T. (1996) *J. Exp. Med.* 178, 389–398.
12. Mohamadizadeh, M., Ariizumi, K., Sugamura, K., Bergstresser, P. R., and Takashima, A. (1996) *Eur. J. Immunol.* 26, 156–160.
13. Reinecker, H.-C., and Podolsky, D. K. (1995) *Proc. Natl. Acad. Sci. U.S.A.* 92, 8353–8357.
14. Bazan, J. F. (1990) *Proc. Natl. Acad. Sci. U.S.A.* 87, 6934–6938.
15. Chi-Rosso, G., Gotwals, P. J., Yang, J., Ling, L., Jiang, K., Chao, B., Baker, D. P., Burkly, L. C., Fawell, S. E., and Kotliansky, V. E. (1997) *J. Biol. Chem.* 272, 31447–31452.
16. Noguchi, M., Adelstein, S., Cao, X., and Leonard, W. J. (1993) *J. Biol. Chem.* 268, 13601–13608.
17. Noguchi, M., Yi, H., Rosenblatt, H. M., Filipovich, A. H., Adelstein, S., Modi, W. S., McBride, O. W., and Leonard, W. J. (1993) *Cell* 73, 147–157.
18. Leonard, W. J., Shores, E. W., and Love, P. E. (1995) *Immunol. Rev.* 148, 97–114.
19. Pepper, A. E., Buckley, R. H., Small, T. N., and Puck, J. M. (1995) *Am. J. Hum. Genet.* 57, 564–571.
20. Puck, J. M., Pepper, A. E., Henthorn, P. S., Candotti, F., Isakov, J., Whitwam, T., Conley, M. E., Fischer, R. E., Rosenblatt, H. M., Small, T. N., and Buckley, R. H. (1997) *Blood* 89, 1968–1977.
21. O'Maricaigh, A. S., Puck, J. M., Pepper, A. E., De Santes, K., and Cowan, M. J. (1997) *J. Clin. Immunol.* 17, 29–33.
22. Clark, P. A., Lester, T., Genet, S., Jones, A. M., Hendricks, R., Levinsky, R. L., and Kinnon, C. (1995) *Hum. Genet.* 96, 427–432.
23. Ishii, N., Asao, H., Kimura, Y., Takeshita, T., Nakamura, M., Tsuchiya, S., Konno, T., Maeda, M., Uchiyama, T., and Sugamura, K. (1994) *J. Immunol.* 153, 1310–1317.
24. Cao, X., Shores, E. W., Hu-Li, J., Anver, M. R., Kelsall, B. L., Russell, S. M., Drago, J., Noguchi, M., Grinberg, A., Bloom, E. T., Paul, W. E., Katz, S. I., Love, P. E., and Leonard, W. J. (1995) *Immunity* 2, 223–238.
25. He, Y.-W., Nakajima, H., Leonard, W. J., Adkins, B., and Malek, T. R. (1997) *J. Immunol.* 158, 2592–2599.
26. Sugamura, K., Asao, H., Kondo, M., Tanaka, N., Ishii, N., Nakamura, M., and Takeshita, T. (1995) *Adv. Immunol.* 59, 225–277.
27. Nakamura, Y., Russell, S. M., Mess, S. A., Friedmann, M., Erdos, M., Francois, C., Jacques, Y., Adelstein, S., and Leonard, W. J. (1994) *Nature* 369, 330–333.
28. Nelson, B. H., Lord, J. D., and Greenberg, P. D. (1994) *Nature* 369, 333–336.
29. Kawahara, A., Minami, Y., and Taniguchi, T. (1994) *Mol. Cell. Biol.* 14, 5433–5440.
30. Smith, K. A., Baker, P. E., Gillis, S., and Ruscetti, F. W. (1988) *Mol. Immunol.* 17, 579–589.
31. Boise, L. H., Minn, A. J., June, C. H., Lindsten, T., and Thompson, C. B. (1995) *Proc. Natl. Acad. Sci. U.S.A.* 92, 5491–5495.
32. Caligiuri, M., Zmuidzinas, A., Manley, T. J., Levine, H., Smith, K. A., and Ritz, J. (1990) *J. Exp. Med.* 171, 1509–1526.
33. Voss, S. D., Robb, R. J., Weil-Hillman, G., Hank, J. A., Sugamura, K., Tsudo, M., and Sondel, P. M. (1990) *J. Exp. Med.* 172, 1101–1114.
34. Tilley, J. W., Chen, L., Fry, D. C., Emerson, S. D., Powers, G. D., Biondi, D., Varnell, T., Trilles, R., Guthrie, R.,

- Mennona, F., Kaplan, G., LeMahieu, R. A., Carson, M., Han, R.-J., Liu, C.-M., Palermo, R., and Ju, G. (1997) *J. Am. Chem. Soc.* 119, 7589–7590.
35. Waldmann, T. A. (1993) *Immunol. Today* 14, 264–270.
36. Hakimi, J., Mould, D., Waldman, T. A., Queen, C., Anasetti, C., and Light, S. (1997) *Antibody Therapeutics* (Harris, W. J., and Adair, J. R., Eds.) CRC Press, Boca Raton, FL.
37. Landgraf, B. E., Williams, D. P., Murphy, J. R., Smith, K. A., and Ciardelli, T. L. (1991) *Proteins: Struct., Funct., Genet.* 9, 207–216.
38. Landgraf, B. E., Goldstein, B., Williams, D. P., Murphy, J. R., Sana, T. R., Smith, K. A., and Ciardelli, T. L. (1992) *J. Biol. Chem.* 267, 18511–18519.
39. Sana, T. R., Wu, Z., Smith, K. A., and Ciardelli, T. L. (1994) *Biochemistry* 33, 5838–5845.
40. Raskin, N., Jakubowski, A., Douglas Sizing, I., Olson, D. L., Kalled, S. L., Hession, C. A., Benjamin, C. D., Baker, D. P., and Burkly, L. C. (1998) *J. Immunol.* (in press).
41. Hatakeyama, M., Tsudo, M., Minamoto, S., Kono, T., Doi, T., Miyata, T., Miyasaka, M., and Taniguchi, T. (1989) *Science* 244, 551–556.
42. Seed, B. (1987) *Nature* 329, 840–842.
43. Gill, S. C., and von Hippel, P. H. (1989) *Anal. Biochem.* 182, 319–326.
44. Coligan, J. E., Kruisbeek, A. M., Margulies, D. H., Shevach, E. M., and Strober, W. (1991) *Purification of Immunoglobulin G, Current Protocols in Immunology* (Coico, R., Ed.) Vol. 1, Wiley-Interscience, New York.
45. Myszka, D. G., Arulanantham, P. R., Sana, T., Wu, Z., Morton, T. A., and Ciardelli, T. L. (1996) *Protein Sci.* 5, 2468–2478.
46. Karlsson, R., Michaelsson, A., and Mattsson, L. (1991) *J. Immunol. Methods* 145, 229–240.
47. Hoffman, R. C., Castner, B. J., Gerhart, M., Gibson, M. G., Rasmussen, B. D., March, C. J., Weatherbee, J., Tsang, M., Gustchina, A., Schalk-Hihi, C., Reshetnikova, L., and Wlodawer, A. (1995) *Protein Sci.* 4, 382–386.
48. Hoffman, R. C., Castner, B. J., Gerhart, M., Gibson, M. G., Rasmussen, B. D., March, C. J., Weatherbee, J., Tsang, M., Gustchina, A., Schalk-Hihi, C., Reshetnikova, L., and Wlodawer, A. (1997) *Protein Sci.* 6, 494.
49. Cao, X., Kozak, C. A., Liu, Y.-J., Noguchi, M., O'Connell, E., and Leonard, W. J. (1993) *Proc. Natl. Acad. Sci. U.S.A.* 90, 8464–8468.
50. Johnson, K., Choi, Y., Wu, Z., Ciardelli, T., Granzow, R., Whalen, C., Sana, T., Pardee, G., Smith, K., and Creasey, A. (1994) *Eur. Cytokine. Netw.* 5, 23–34.
51. Damjanovich, S., Bene, L., Matko, J., Alileche, A., Goldman, C. K., Sharrow, S., and Waldmann, T. A. (1997) *Proc. Natl. Acad. Sci. U.S.A.* 94, 13134–13139.
52. Gonzalez-Garcia, A., Merida, I., Martinez-A, C., and Carrera, A. (1997) *J. Biol. Chem.* 272, 10220–10226.
53. Smith, K. A. (1988) *Science* 240, 1169–1176.
54. Doherty, P. C. (1993) *Cell* 75, 607–612.
55. Steiger, J., Nickerson, P. W., Steurer, W., Moscovitch-Lopatin, M., and Strom, T. B. (1995) *J. Immunol.* 155, 489–498.
56. Manfro, R. C., Roy-Chaudhury, P., Zheng, X. X., Steiger, J., Nickerson, P. W., Li, Y., Maslinski, W., and Strom, T. B. (1997) *Transplant Proc.* 29, 1077–1078.

BI981355M